6ICEGE 6th International Conference on Earthquake Geotechnical Engineering
1-4 November 2015
Christchurch. New Zealand

An Investigation on the Variation of Mechanical Properties of Saturated Sand During Liquefaction

Y-Y.Ko[1], C-H. Chen[2], T-S. Ueng[3], C-H. Chen[4]

ABSTRACT

Soil liquefaction not only induces settlement and lateral spreading of the ground, but also lowers the stiffness and strength of the soil body. In order to investigate the variation of soil mechanical properties during liquefaction, data of the shaking table tests on saturated sand using a large laminar shear box conducted in National Center for Research on Earthquake Engineering were analyzed. Firstly, the excited responses of saturate soil during liquefaction were characterized. Furthermore, one-dimensional shear beam idealization was adopted to establish the simplified soil profile model, and system identification of the soil body can thus be conducted to examine the variation of mechanical properties of saturated sand, such as the shear modulus and the damping ratio, with respect to the development of shear strain and excess pore water pressure. Results of this study will be helpful to assess the real seismic behavior of liquefied soil.

Introduction

Taiwan locates in the seismic active west Pacific Rim, and therefore earthquake disasters are inevitable. In Taiwan, population are concentrated in alluvial plains, and thus soil liquefaction is the threat that people in Taiwan have to face. Soil liquefaction causes not only the settlement and lateral spreading of sandy ground, but also the reduction of the stiffness and strength of the sandy soil. Consequently, the seismic behavior and the aseismic capacity of the foundation and other engineering structures resting on liquefied soil will be influenced. Therefore, the weakening of soil induced by liquefaction should be appropriately considered in seismic design.

In Taiwan, the reduction factors for the mechanical parameters of liquefied soil proposed in JRA (1996) and in AIJ (1998) are widely used in foundation design. However, these reduction factors are not based on solid theories and are inconsistent. Because existing related studies are quite limited, conservative considerations are usually adopted in engineering practice, causing uneconomical designs. Therefore, it is necessary to investigate the variation of soil mechanical properties during liquefaction for a real assessment of the seismic behavior of liquefied soil and for more reasonable seismic design.

In order to effectively simulate the seismic response of layered soil, National Center for Research on Earthquake Engineering (NCREE) developed a large biaxial laminar shear box with

[1]Associate Researcher, Nat'l Center for Research on Earthquake Engng., Taipei, Taiwan, yyko@ncree.narl.org.tw
[2]Assistant Researcher, Nat'l Center for Research on Earthquake Engng., Taipei, Taiwan, chiaham@ncree.narl.org.tw
[3]Professor Emeritus, Department of Civil Engng., National Taiwan University, Taipei, Taiwan, ueng@ntu.edu.tw
[4]Professor, Department of Civil Engng., National Taiwan University, Taipei, Taiwan, chchen2@ntu.edu.tw

a inner dimension of 1.88 m (L) × 1.88 m (W) × 1.52 m (H) (Ueng et al., 2006a), as shown in Figure 1(a). To allow biaxial motion, each layer consists of an inner and an outer frames able to move in two orthogonal directions respectively in the horizontal plane, as shown in Figure 1(b), and each layer can move independently so that the box can provide a laminar flexible boundary to minimize the boundary effect. Along with the large shaking table of NCREE, large scale geotechnical physical model tests can be performed, making the seismic response of the soil specimen be more similar to the real situation. In order to study the characteristics of liquefaction behavior of saturated sand, a series of physical model shaking table test were conducted in NCREE in 2002~2007 using this shear box (Ueng et al., 2006b; Ueng et al., 2008).

In this research, these experimental data were utilized o investigate the variation of mechanical properties of saturated sand during the process of liquefaction. Firstly, the excited responses of saturate soil were characterized in each stage of liquefaction. In addition, one-dimensional shear beam idealization was adopted to establish the simplified soil profile model for the system identification of the soil body, and then the variation of soil mechanical properties with respect to the development of shear strain and excess pore water pressure can thus be examined.

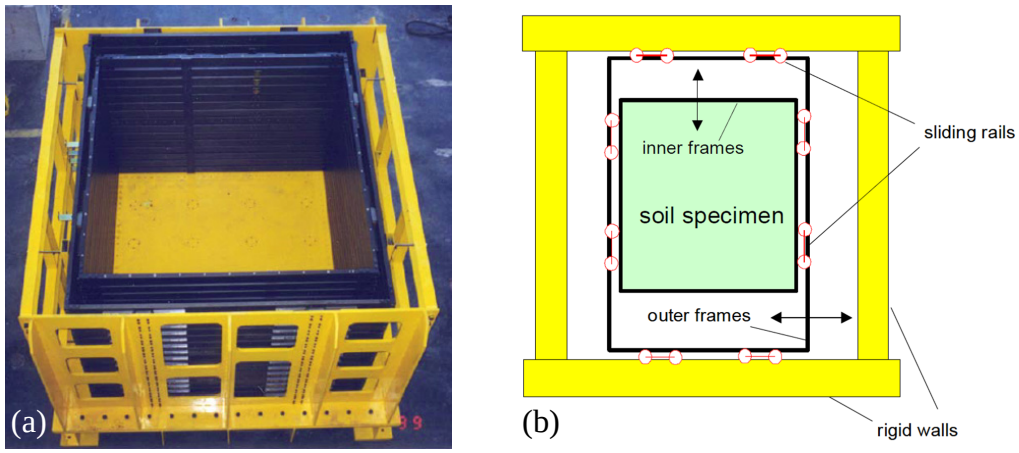

Figure 1. NCREE laminar shear box: (a) top view (b) movable frame scheme (Ueng et al., 2006b)

Literature Review of Influence of Liquefaction on Mechanical Properties of Soil

Kostadinov and Towhata (2002) performed time-frequency analysis on the earthquake records of several liquefied sites using short-time Fourier transform (STFT) to investigate the change of the mean instantaneous frequency (MIF) of the ground seismic response. The MIF of each site was significantly lowered after liquefaction. Kramer et al. (2011) also conducted time-frequency analysis on earthquake records of liquefied sites using STFT, wavelet transform and Stockwell transform. Dramatic reduction in acceleration amplitude and predominant frequency were observed, showing that the liquefaction induced the quick softening of soil.

In order to study the dynamic behavior of soil in a well controlled environment, small scale laboratory tests are often adopted. Seed and Lee (1966) were the pioneers using the cyclic triaxial test to investigate the liquefaction of saturated sand, and indicated that effective stresses

of soil will be nearly zero. Martin et al. (1975) depicted that the shear stress, as well as the shear modulus of soil, is proportional to the square root of vertical effective stress based on laboratory tests to characterize the volumetric change of sand subjected to cyclic shear. Hence, decrease of vertical effective stress will degrade the shear modulus. This is conformable to the observations from the earthquake records of liquefied sites. Kokusho (1980) also verified that the idea of Martin et al. (1975) was valid in small strains using drained cyclic triaxial tests.

If the variation of soil mechanical properties can be estimated according to actual earthquake records, the real seismic behavior of soil in field can be more authentically reflected. A simple idea of one-dimensional (1-D) shear beam idealization proposed by Koga and Matsuo (1990) was utilized by Zeghal and Elgamel (1994) to obtain shear stress-strain histories within the ground profile in 1987 Superstition Hills Earthquake based on the data of the downhole accelerometer array at Wildlife Refuge, California. This earthquake caused a significant increase of excess pore water pressure, and evidences of liquefaction such as sand boils and minor lateral spreading were observed in field investigations. According to the analysis results, the shear wave velocity was obviously reduced as the sharp rise of excess pore water pressure occurred.

System Identification Using 1-D Shear Beam Idealization

Considering the case that shear horizontal (SH) waves propagate vertically in horizontally layered soil, the 1-D shear beam theory can be used for the idealization of the soil profile. Then, using the idea proposed by Koga and Matsuo (1990), the shear stress-strain histories of the soil body can be calculated from the measured ground response (displacement or acceleration), and the soil mechanical properties can be accordingly estimated. As shown in Figure 2, the soil profile is idealized as a 1-D shear beam and is discretized. Then the shear stress time history of the soil body at a depth of h can be expressed via the mass density of soil, ρ, and the soil acceleration at a depth of x, $\ddot{u}(x)$, as $\tau(h,t)=\int_0^h \rho\ddot{u}(x)dx$. Then, If the accelerations at the black points in Figure 2 are known, the shear stress at the i-th point (at a depth of x_i) can be calculated:

$$\tau_i(t)=\tau_{i-1}(t)+\rho\frac{\ddot{u}_{i-1}+\ddot{u}_i}{2}(x_i-x_{i-1}) \tag{1}$$

where $\tau_i(t)=\tau(x_i,t)$, and $\ddot{u}_i=\ddot{u}(x_i,t)$. In addition, the shear strain at a depth of x_i can be calculated in the finite difference form:

$$\gamma_i(t)=\frac{1}{\Delta x_i+\Delta x_{i-1}}\left\{\left[u_{i+1}(t)-u_i(t)\right]\frac{\Delta x_{i-1}}{\Delta x_i}+\left[u_i(t)-u_{i-1}(t)\right]\frac{\Delta x}{\Delta x_{i-1}}\right\} \tag{2}$$

where $\Delta x_i=x_{i+1}-x_i$.

Thus, because $\tau_1(0)=0$ (free surface condition), the shear stresses at different depths can be calculated subsequently using Equation 1 from the accelerations at different depths. Also, the shear strains can be calculated using Equation 2 from the directly measured displacements or the double time integration of accelerations. Consequently, the hysteretic loop of the stress-strain time histories can be obtained, and the equivalent linear shear modulus G_{eq} and hysteretic damping ratio β can be accordingly estimated, as shown in Figure 3.

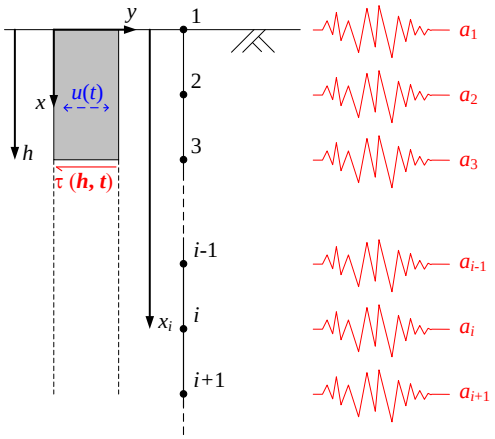

Figure 2. 1D shear beam idealization.

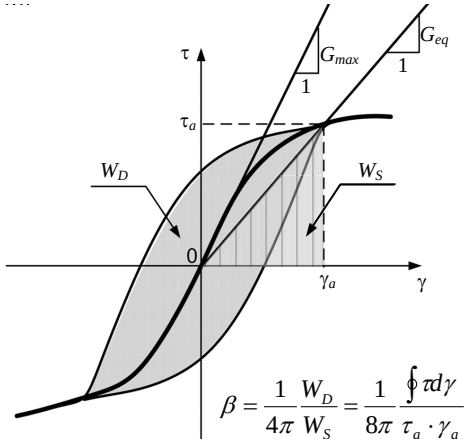

Figure 3. Stress-strain hysteretic loop.

Case Study- Sinusoidal Excitation Test of Saturated Sand

The large shaking table tests of NCREE on saturated Vietnam sand (Ueng et al., 2006b), which is often regarded as clean sand, was utilized for case study. In order to clearly characterize the seismic behavior of the soil, one of the horizontal uniaxial sinusoidal excitation test was adopted. The input motion was a 2-Hz sinusoidal wave with an amplitude of 0.075 g. An accelerometer was installed within the soil body at a depth of 556 mm below the soil surface and about at the center horizontally. At the same location a piezometer was installed. Accelerometers and variable differential transformers (LVDTs) were also installed on movable frames of the shear box. Thus, the method mentioned in the previous section can be applied to analyze the test data.

Characteristics of Excited Responses of Saturate Sand

Figure 4 shows the measured accelerations of the soil body at a depth of 556 mm and the frame of the shear box at the same elevation, and excess pore water pressure. The pore water pressure increased sharply during 2~4 sec, and reached a upper bound at 5 sec. At about 4 sec the response of the soil body started to change, implying the initial liquefaction had occurred. After the initiation of liquefaction (4~5 sec), the acceleration showed a significant spike and then exhibited a response with a longer period. Afterwards, the acceleration amplitude reduced obviously and showed a multi-frequency curve, representing complete liquefaction. Concerning the frame, a high frequency response was observed after liquefaction, which could be related to the significant stiffness decrease of liquefied soil, which not only altered the vibration characteristics of soil body, but also induced the high frequency vibration of frames due to the loss of lateral resistance.

Stress-Strain Hysteretic Loop of Soil Response

According to the previous section, spectral analysis can exhibit the degradation of f_{pre} of soil response during liquefaction, and can also clarify the unexpected response resulted from test setup. However, due to the resolution of spectrum and environmental conditions, spectral analysis is more appropriate for qualitative investigation of the seismic behavior of liquefied soil rather than quantitative description. Hence, the 1-D shear beam idealization (Koga and Matsuo,

1990) mentioned previously was further introduced to deduce the time histories of the shear stress and shear strain of the soil body during excitation. Thus, the stress-strain hysteretic loop can be obtained, and the shear modulus and damping ratio can be estimated based on Figure 3.

Utilizing Equation 1 and Equation 2, the time history of shear stress and shear strain of the soil body can be calculated from the data of the accelerometer within the soil body and the data of LVDT at the frames near the observed elevation. Accordingly, the stress-strain hysteretic loop of the soil body was obtained. Figure 5(a) depicts the hysteretic loops before liquefaction (0~4 sec), in which it can be observed that the slope declined and the area enlarged significantly, implying the degradation of the soil stiffness and the increase of the damping ratio. From the hysteretic loops after liquefaction (4~8 sec), as shown in Figure 5(b), it is found that the slope dropped to a very low value after the maximum of shear stress was reached, indicating that the soil had scarce any stiffness. However, the soil still had the capability of energy dissipation because the hysteretic loops had considerable area . In addition, it should be mentioned that the shear strain developed rapidly between 2~4 sec (as excess pore water pressure increased quickly) and reached a maximum at 4.1 sec.

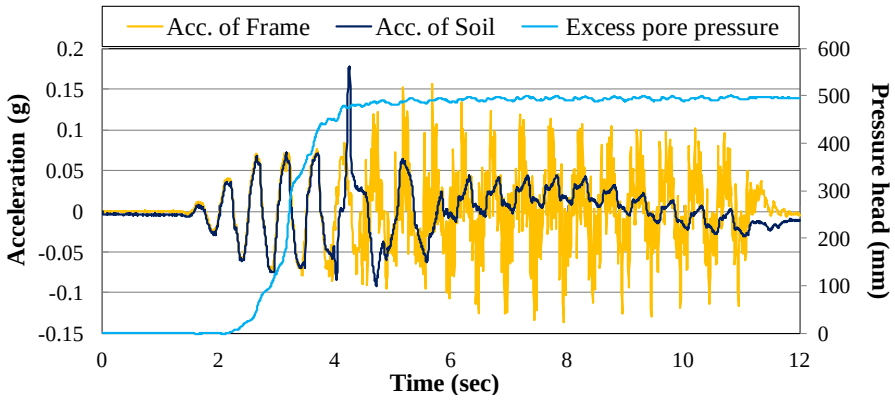

Figure 4. Accelerations of soil body and frame and excess pore water pressure (depth = 556 mm).

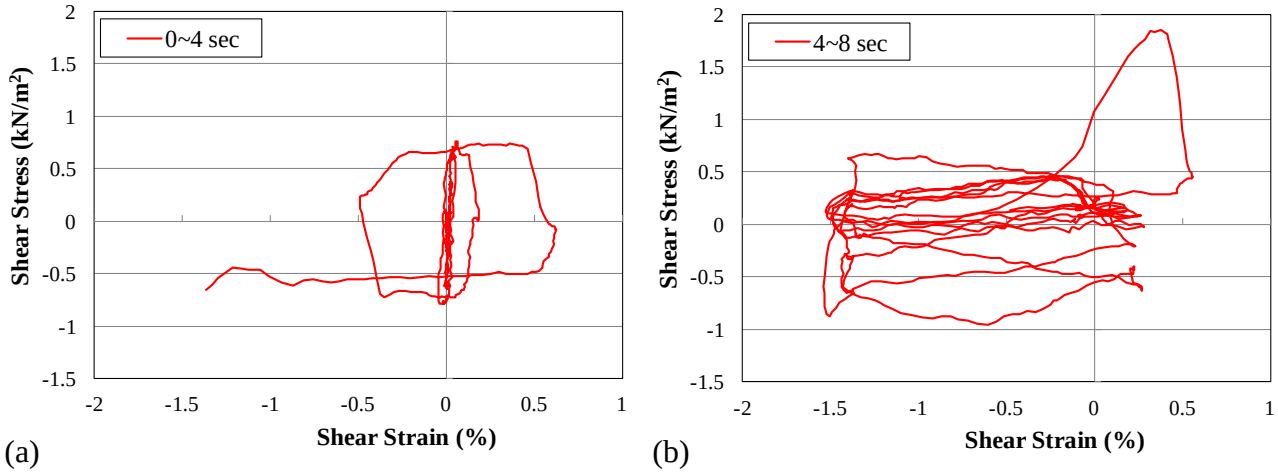

(a) (b)

Figure 5. Stress-strain hysteretic loop of the soil body: (a) 0~4 sec; (b) 4~8 sec.

Variation of Mechanical Properties of Saturated Sand During Liquefaction

From Figure 5, it is noticed that the variation of soil mechanical properties during liquefaction occurred primarily in the process of the generation of excess pore water pressure and the development of shear strain. Therefore, the stress-strain hysteretic loops in the duration when excess pore water pressure and shear strain changed most significantly (2.1~4.1 sec) were used to estimate the shear moduli and compare them to the corresponding excess pore water pressures, as shown in Figure 6. The equivalent shear modulus G_{eq} generally decreased as the excess pore water pressure ratio (r_u, ratio of excess pore water pressure to vertical effective stress) increased, and was nearly zero when r_u was over 0.8, indicating that completely liquefied soil can be considered having no stiffness. It is also found that G_{eq} showed an exponential decay with respect to r_u. However, r_u was actually dependent on shear strain amplitude (γ_{amp}) and showed a logarithmic relationship, as shown in Figure 7. Consequently, the degradation of shear modulus was actually influenced by shear strain and excess pore water pressure simultaneously.

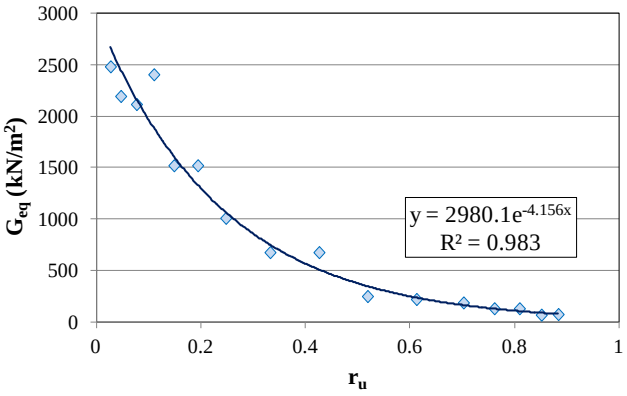

Figure 6. Relationship between G_{eq} and r_u.

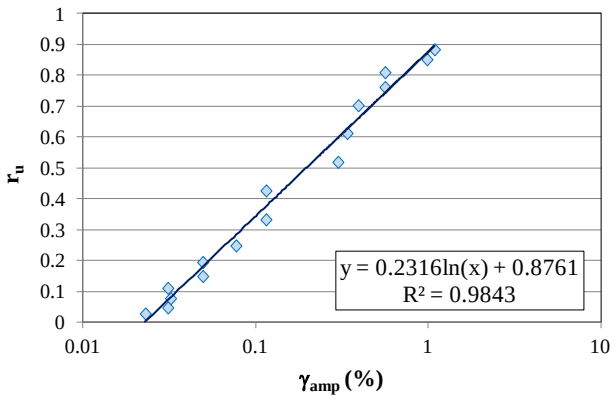

Figure 7. Relationship between r_u and γ_{amp}.

The relationship between the normalized shear modulus ratio (G_{eq}/G_0, where G_0 denotes the shear modulus corresponding to a shear strain of 10^{-6}) and the effective strain γ_{eff} (γ_{eff} = $0.65\gamma_{amp}$) obtained in this study is given in Figure 8. It was compared with the shear modulus degradation curve proposed by Seed and Idriss (1970), which was mainly based on experimental data on clean sand, has been considered representative and was specified as the default for sand in the ground response analysis code SHAKE 91 (Idriss and Sun, 1992). It should be mentioned that the G_{eq}/G_0 value related to the minimum γ_{eff} of this study (when r_u was nearly zero) was assumed to be identical of the G_{eq}/G_0 value of Seed and Idriss (1970) at the same γ_{eff} value. It is noted that both decreased with respect to γ_{eff} with a similar decaying tendency, yet considerable difference was observed when the strain level was higher. G_{eq}/G_0 of this study was smaller, probably due to the influence of the excess pore water pressure. In addition, Figure 9 exhibits relationship between the damping ratio β and γ_{eff}, and it was compared with that proposed by Idriss (1990) for clean sand, which was also used as the default for sand in SHAKE 91. Both damping ratio curves increased with respect to γ_{eff} yet the data in the one of this study were much more dispersed, and were larger due to the effect of excess pore water pressure.

Because Figure 8 can be considered for the drained condition, it can be used to eliminate the effect of shear strain in Figure 6 by introducing the relationship given in Figure 7. Thus, the relationship between G_{eq} and r_u without the influence of shear strain can be obtained, as given in Figure 10(a), which still showed an exponential decay trend as in Figure 6. In a similar way, the relationship between β and r_u with the effect of shear strain eliminated can be acquired, as shown in Figure 10(b), which was roughly a logarithmic relationship yet was rather fluctuated. However, it can still be noted that the excess pore water pressure due to the sinusoidal excitation to the soil caused a considerable rise of the damping ratio ranged between 10%~30%.

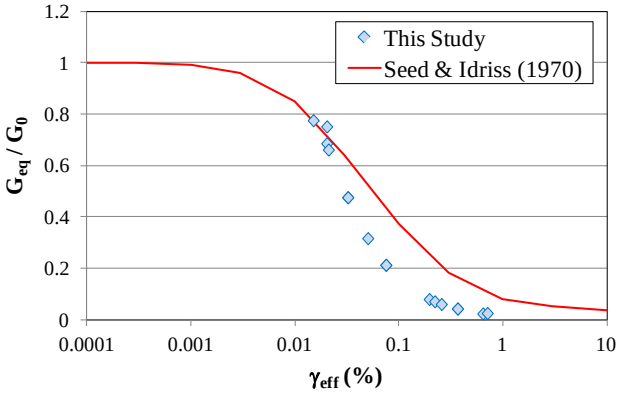

Figure 8. Shear modulus vs. shear strain.

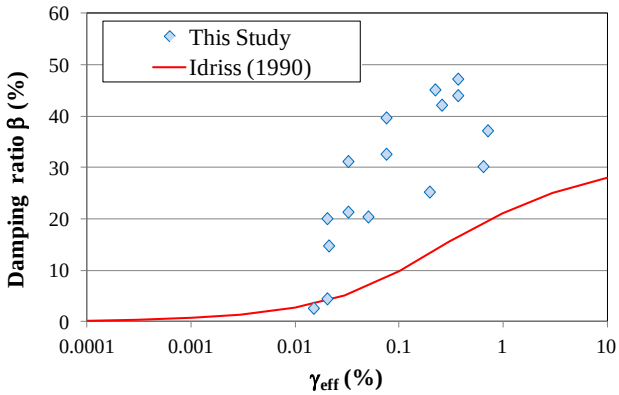

Figure 9. Damping ratio vs. shear strain.

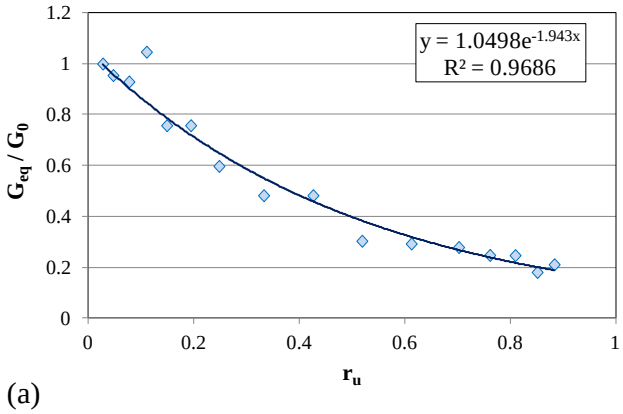

(a)

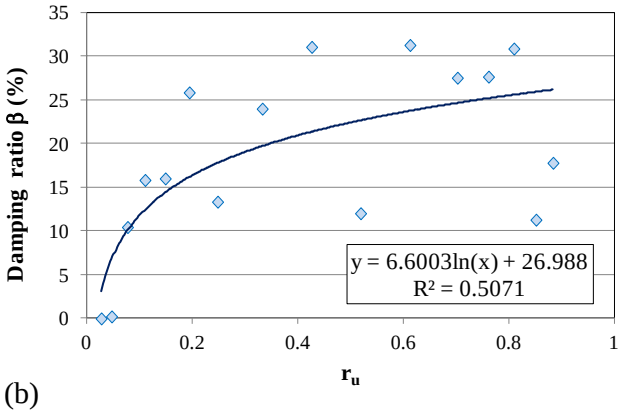

(b)

Figure 10. Relationships with the effect of shear strain eliminated: (a) G_{eq}/G_0 vs. r_u; (b) β vs. r_u.

Conclusions

1. The softening of soil after liquefaction due to the decrease of effective stresses can be noted from the accelerations of soil body and the frame of shear box in the sinusoidal excitation test.
2. Stress-strain hysteretic loops of the soil in the sinusoidal excitation test can be obtained using the 1-D shear beam idealization, and the decrease of stiffness and the increase of damping during the development of liquefaction can be accordingly observed.
3. Based on the system identification of the soil body using its stress-strain hysteretic loops, the relationships of decline of shear modulus and the rise of hysteretic damping ratio with respect

to the shear strain can be obtained. Comparing these relationships to the often used curves of soil mechanical properties versus shear strain, the influence of excess pore water pressure on the decrease of shear modulus and the increase of damping ratio can be exhibited.

4. Using the change of excess pore water pressure versus the shear strain, the effect of shear strain can be eliminated to obtain the variation curves of shear modulus and damping ratio with respect to the excess pore water pressure ratio, which can serve as the reference of seismic design and analysis in engineering practice.

Acknowledgments

The authors express their gratitude for the financial support provided by Ministry of Science and Technology, Executive Yuan, Taiwan.

References

Architectural Institute of Japan (AIJ). *Recommendations for Design of Building Foundations*. Architectural Institute of Japan: Tokyo, 1988 (in Japanese) .

Idriss IM. Response of soft soil sites during earthquakes. *Proceedings of Symposium to Honor Professor H.B. Seed*. University of California: Berkeley, CA, 1990: 273-289.

Idriss, IM, Sun, JI, *User's Manual for SHAKE91*. University of California, Davis: Davis, CA, 1992.

Japan Road Association (JRA). *Design Specifications for Highway Bridges*. Japan Road Association: Tokyo, 1996 (in Japanese).

Koga Y, Matsuo O. Shaking table tests of embankments resting on liquefiable sandy ground. *Soils and Foundations* 1990; **30**(4): 162-174.

Kokusho, T. Cyclic triaxial test of dynamic soil properties for wide strain range. *Soils and Foundations* 1980, **20** (2): 45-60.

Kostadinova MV, Towhata I. Assessment of liquefaction-inducing peak ground velocity and frequency of horizontal ground shaking at onset of phenomenon. *Soil Dynamics and Earthquake Engineering* 2002; **22**(4): 309-322.

Kramer SL, Hartvigsen AJ, Sideras SS, Ozener PT. Site response modeling in liquefiable soil deposits. *4th IASPEI / IAEE International Symposium: Effects of Surface Geology on Seismic Motion* 2011: Santa Barbara, CA.

Martin, GR, Finn WDL, Seed HB. Fundamentals of liquefaction under cyclic loading. *Journal of the Geotechnical Engineering Division*, ASCE 1975; **101(**5): 423-438.

Seed HB, Idriss IM. *Soil Moduli and Damping Factors for Dynamic Response Analysis*. Report No. EERC 70-10. Earthquake Engineering Research Center: Berkeley, CA, 1970.

Seed HB, Lee KL. Liquefaction of saturated sands during cyclic loading. *Journal of the Soil Mechanics and Foundations Division* 1966; **92**(6): 105-134.

Ueng TS, Wang MH, Chen MH, Chen CH, and Peng LH. A large biaxial shear box for shaking table tests on saturated sand. *Geotechnical Testing Journal* 2006, 29 (1):1-8.

Ueng TS, Chen CH, Cheng HW, Wu CW. *Large-Scale Shear Box Soil Liquefaction Tests on Shaking Table (III) - Settlement of Saturated Vietnam Sand Specimen in Shaking Table Tests*. Research Report NCREE-06-019. National Center for Research on Earthquake Engineering: Taipei, 2006.

Ueng TS, Chen CH, Tsou CF, Chen YC. *Large-Scale Shear Box Soil Liquefaction Tests on Shaking Table (IV) - Behaviors of Saturated Mailiao Sand Specimen in Shaking Table Tests*. Research Report NCREE-08-011. National Center for Research on Earthquake Engineering: Taipei, 2008.

Zeghal M, Elgamel AW. Analysis of site liquefaction using earthquake records. *Journal of Geotechnical Engineering*, ASCE 1994; **120**(6): 996-1017.